

Mechanochemically assisted solid state synthesis and catalytic properties of CuWO₄

M. N. Gancheva*, P. M. Konova, G. M. Ivanov, L. I. Aleksandrov, R. S. Iordanova, A. I. Naydenov

*Institute of General and Inorganic Chemistry, Bulgarian Academy of Science,
Acad. G. Bonchev St., Bldg. 11, 1113 Sofia, Bulgaria*

Received: January 16, 2018; Revised: April 26, 2018

The synthesis and catalytic properties of nanostructured copper tungstate have been investigated in this study. A mixture of CuO and WO₃ at a molar ratio of 1:1 was subjected to intensive mechanical treatment in air using a planetary ball mill for different periods of time. Structural and phase transformations were monitored by X-ray diffraction analysis, differential thermal analysis, and infrared spectroscopy. Mechanochemical treatment promoted progressive amorphisation of the initial oxides. Full amorphisation was achieved after 7 h milling time and remained up to 20 h milling time. DTA measurements of amorphous sample showed that the crystallization temperature was 430 °C. A pure nanostructured CuWO₄ phase was prepared after thermal treatment of amorphous phase at 400 °C. Nanostructured CuWO₄ was tested in the reactions of complete oxidation of C₁-C₄ hydrocarbons and the highest temperature for 10% conversion (T₁₀) was measured with methane. Repeated addition of one further carbon atom to the methane molecule led to a decrease in T₁₀ by about 70 °C (from methane to propane) and further by 30 °C from propane to *n*-butane. Calculated apparent activation energies for the reaction of complete oxidation decreased from methane to *n*-butane, and this effect correlated with diminished strength of the weakest C-H bond of the corresponding hydrocarbon.

Key words: mechanochemistry, nanoparticles, catalytic activity, preparation of single phase CuWO₄.

INTRODUCTION

CuWO₄ is a member of metal tungstate oxides (AWO₄) group, which have received much attention due to their application in various fields as catalysts [1–3], optical devices [4], sensors [5], and magnetic properties [6]. AWO₄ (A = Ni, Fe, Zn, and Cu) tungstate family oxides exhibit a wolframite-type of monoclinic structure, where both A and W atoms are bonded to six surrounding oxygen atoms by forming octahedral chains [7]. Like-filled octahedra share edges, but unlike octahedra share vertex. In this way edge-sharing distorted WO₆ octahedra form W₂O₈ structural units. Among these tungstates only CuWO₄ crystallizes in a triclinic wolframite-type of structure at room temperature composed by CuO₆ and WO₆ octahedra distorted by the first-order and second-order Jahn-Teller effects, respectively [8–10]. Some authors have suggested that the CuO₆ octahedra possess a pseudo-tetragonally elongated geometry [10,11]. Ruiz-Fuertes *et al.* [12] have established that CuWO₄ undergoes phase transition from a low temperature triclinic phase to a monoclinic one with wolframite-type of structure at 10 GPa involving a change in the magnetic order. Different methods for CuWO₄ preparation as sol-gel [5], coprecipitation [2,4,10], solid state reaction [10,11], sonochemistry [3], microwave-assisted syn-

thesis [13], polyol-mediated approach [1], electrochemical synthesis [14], and hydrothermal route [5,15,16] have been developed. There are some disadvantages concerned with metal salts used as raw materials (necessity of anion removal), strictly controlled synthesis media, high costs, and thermal treatment after synthesis. Up to now, mechanochemical synthesis of CuWO₄ compound from initial oxides has not been studied. It is well known that the mechanochemical activation is a suitable method for preparation of complex inorganic oxides [16–18]. It is characterized by lower synthesis temperature, chemical homogeneity, high purity, and sample crystallite size and morphology control. Careful regulation of milling parameters is a promising way to improve the physicochemical properties of the final products as compared to conventional routes. We have found out that ball milling is an appropriate approach to synthesis different inorganic materials like ZnO, NiWO₄, ZnWO₄, ZrMo₂O₈, Bi₂WO₆, and MgWO₄ [19–24]. Our investigations showed that metal tungstates (MgWO₄ and Bi₂WO₆) obtained by mechano-chemical activation exhibit a moderate catalytic activity for oxidation of CO and volatile organic compounds (VOCs) [23,24]. This motivated us to continue experiments in the same field. The aim of this study was to investigate the catalytic activity of nanopowder CuWO₄ prepared *via* mechanochemically assisted solid-state synthesis.

* To whom all correspondence should be sent
E-mail: m.gancheva@svr.igic.bas.bg

EXPERIMENTAL

CuO (Merck, 99.9%) and WO₃ (Aldrich, 99.9%) starting materials at a molar ratio of 1:1 were subjected to intense mechanical treatment using a planetary ball mill (Fritsch-Premium line-Pulverisette No. 7). Both vials and balls were made of stainless steel. The following milling conditions were used: air atmosphere; milling speed of 500 rpm; ball to powder weight ratio of 10:1, and milling time varying from 0 to 20 h. To avoid excessive temperature rise within the grinding chamber, 15 min of ball milling duration were followed by a pause of 5 min. Milled amorphous samples were heated at 400 °C for 6 h in air atmosphere. X-ray diffraction (XRD) patterns were registered on a Bruker D8 Advance diffractometer using Cu-K α radiation in the 2 θ range of 10–80°. Average crystallite sizes (D) resulting from X-ray diffraction line broadening were determined using Scherrer' equation: $D = K\lambda/\beta\cos\theta$, where D is the crystallite size in nm, K is a constant, conventionally accepted to be 1.0, λ is the Cu-K α radiation wavelength (1.5406 Å), β is the full width at half maximum (FWHM) of the diffraction line, and θ in radians is the corresponding diffraction peak is 2 θ = 19.00°. Differential thermal analysis (DTA) was performed in air by SETARAM LabsysEvo apparatus, at a heating rate of 5 °C.min⁻¹, in an open corundum crucible. Specific surface areas (BET method) were determined by low-temperature (77.4 K) nitrogen adsorption in NOVA 1200e surface area & pore analyzer at relative pressures $p/p_0 = 0.1$ –0.3 using BET equation. Infrared spectra were recorded in the range of 1200–400 cm⁻¹ on a Nicolet-320 FTIR spectrometer using the KBr pellet technique. Catalytic activity tests were carried out in a continuous flow type reactor. The following conditions were applied: catalyst bed volume of 0.5 cm³ (0.3 cm³ catalyst and 0.2 cm³ quartz-glass particles of same size), irregular shaped particles having an average diameter of 0.45 ± 0.15 mm, reactor diameter of 6.0 mm, and quartz-glass ($D_{reactor}/D_{particles} \geq 10$). The gaseous hourly space velocity (GHSV) was fixed to 100 000 h⁻¹. Inlet concentration for each one of the individually tested hydrocarbons (methane, ethane, propane, and butane) was set to 0.10 vol.%, while oxygen supply was kept at 20.0 vol.%. All gas mixtures were balanced to 100% with nitrogen (4.0). Gas analysis was performed using on-line gas-analyzers of CO/CO₂/O₂ (Maihak) and THC-FID (total hydrocarbon content with a flame ionization detector, Horiba). To compensate adiabatic effect of the reaction, the catalyst bed temperature was kept almost constant. Pressure drop of the catalytic bed was measured to be less than 2 kPa

and it was not taken into account. Axial dispersion effect was neglected as the catalyst bed matched a chain of more than 10 ideal mixing cells along the reactor axis. Therefore, the geometrical characteristics and the flow conditions of the catalytic reactor justify a conclusion that the reactor was close to the case of isothermal plug flow reactor (PFR) except for the effect of radial velocity profile inside the catalyst bed.

RESULTS AND DISCUSSION

XRD analysis was used to monitor phase transformation during mechanochemical treatment (Fig. 1). The diffraction lines indexed with monoclinic CuO (JCPDS 01-072-0677) and monoclinic WO₃ (JCPDS 01-072-0677) became broadened and less intense after 1 h milling time (Fig. 1b).

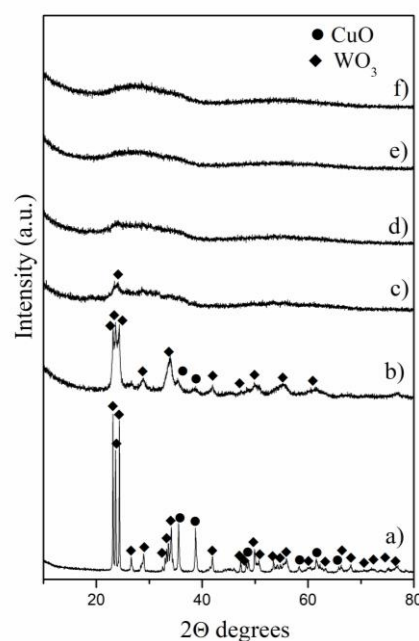


Fig. 1. X-ray diffraction patterns of mechanochemically activated mixture of CuO and WO₃ at: (a) 0 h; (b) 1 h; (c) 3 h; (d) 7 h; (e) 10 h; (f) 20 h.

All reflections of CuO disappeared after 3 h of milling time interval, while reflections of WO₃ were still observed (Fig. 1c). This indicates that CuO amorphisation was easier than that of WO₃. Complete amorphisation of the samples was observed after 7 h milling time (Fig. 1d). Further mechanochemical treatment up to 20 h did not promote chemical reaction and production of any new compound (Fig. 1f). Thermal analysis was used to determine the reaction temperature between mechanochemically activated reagents.

Fig. 2 shows a TG/DTA curve of a sample after 20 h milling time in air atmosphere. The presence of one strong exothermic peak at 430 °C could be

attributed to the formation of CuWO₄. All reflection lines typical of triclinic CuWO₄ (JCPDS-01-080-5325) were observed in the diffraction patterns of amorphous samples heated at 400 °C for 6 h (Fig. 3).

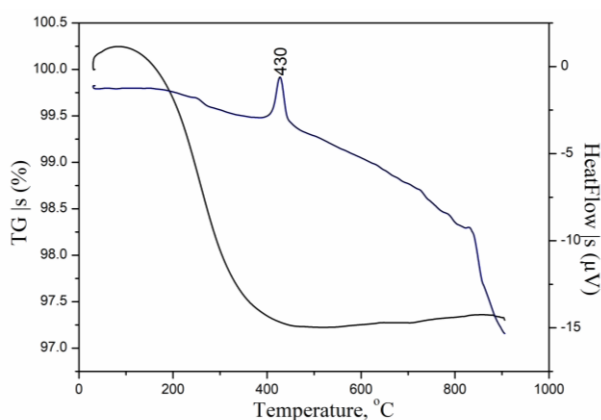


Fig. 2. TG/DTA curves of CuWO₄ sample after 20 h milling time.

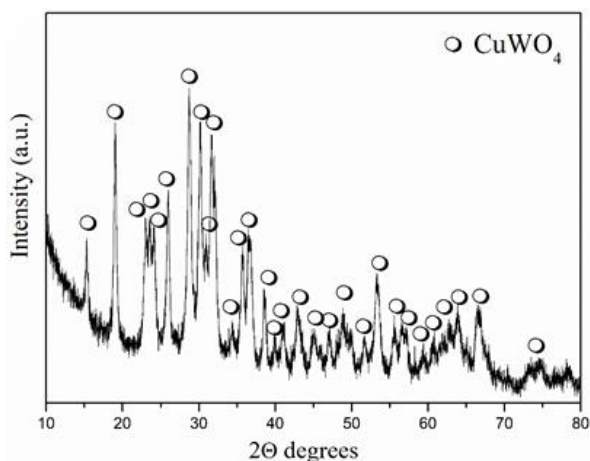


Fig. 3. XRD pattern of CuWO₄.

This temperature was considerably lower as compared to the temperature needed for traditional solid-state reaction (800 °C) [10]. Well-defined diffraction peaks suggest a high degree of crystallinity of the final product. As-prepared CuWO₄ had an average crystallite size of 24 nm according to the Scherrer equation with specific surface area of 13 m²/g.

Structural arrangement during mechanochemical treatment and formation of CuWO₄ were investigated by IR spectroscopy (Fig. 4). IR spectrum of non-activated sample shows the characteristic bands of the initial oxides. The bands at 830 and 780 cm⁻¹ are assigned to stretching vibrations of W–O–W bridge bonds between WO₆ octahedra in WO₃ [25,26]. The absorption bands at 590, 530, and 480 cm⁻¹ are due to a stretching vibration of Cu–O bond of monoclinic CuO phase [27].

Mechanochemical treatment of the sample had strong influence on bands intensity and position.

After 1 h milling time the bands at 780, 590, and 530 cm⁻¹ disappeared, the bands at 840 and 480 cm⁻¹ were broadened, and their intensity was decreased (Fig. 4b). This fact is a result of destruction of the long-range order and partial amorphisation of the reagents. On the other hand a new absorption band at 625 cm⁻¹ appeared that could be attributed to a vibration of Cu–O bond typical of Cu₂O phase [28,29].

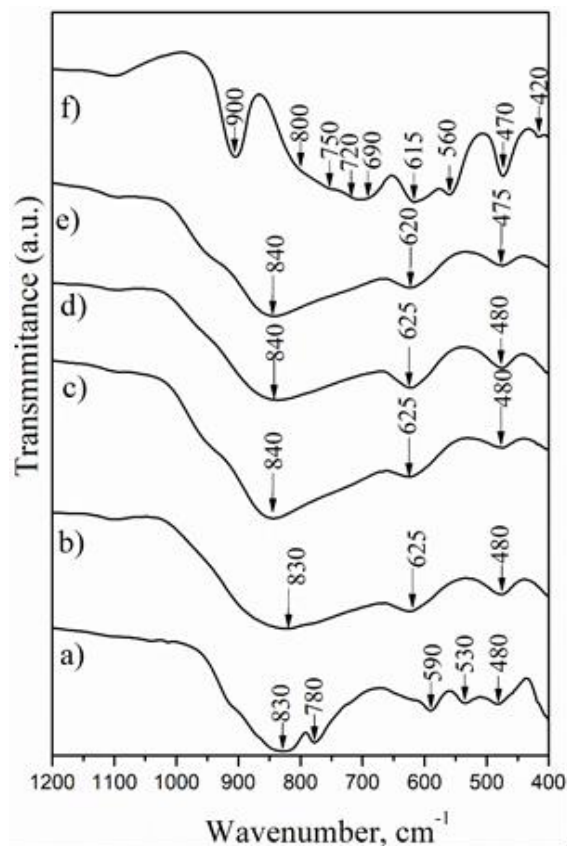


Fig. 4. IR spectra of mechanochemically activated mixture of CuO and WO₃ at: (a) 0 h; (b) 1 h; (c) 3 h; (d) 7 h; (e) 20 h; (f) sample heated at 400 °C after 20 h milling time.

It was established that mechanochemical treatment induced partial transformation of CuO to Cu₂O phase. A similar result has been reported by Sheibani *et al.* [30]. According to the X-ray diffraction analysis sample amorphisation induced by ball milling completed after 7 h milling time and the IR spectrum contains bands at 840, 620, and 480 cm⁻¹ (Fig. 4d–f). Annealing of amorphous sample at 400 °C led to significant changes in the FTIR spectrum. The observed absorption bands are in good agreement with previously reported IR data on this compound [2–4,30,31]. Band assignment was carried out based on structural data on CuWO₄, X-ray absorption fine structure (EXAFS) analysis [6,10,32], and vibration data on AWO₄ (A = Ni, Zn, and Mg) phase of wolframite type of structure [21,24,33,34].

The bands at 800 and 750 cm⁻¹ are due to the vibrations of WO₂ entity present in W₂O₈ groups. The bands at 720, 690, and 615 cm⁻¹ are typical of the asymmetric stretching vibrations of a two-oxygen bridge type species (W₂O₂). The band below 600 cm⁻¹ arises from vibrations of CuO₆ polyhedra [21, 24,33,34].

To examine synthesized CuWO₄ applicability as combustion catalyst, the reactions of complete oxidation of different hydrocarbons (methane, ethane, propane, and butane) were investigated. Reproducibility and confidence intervals for measured conversion values were the subject of preliminary tests, which involved repeating of tests under conditions similar but not identical to separate experimental runs presented in the study. Calculated standard deviation SD = +/-1.5% was based on the average of six measurements for each one of the experimental points. The reported results are based on the average values for conversion degree within two parallel measurements. Data on conversion-temperature dependencies were used to fit kinetics parameters by applying the method described by Duprat [35] and Harriot [36]. In brief, this method consists of direct integration of the reaction rate based on data on temperature-conversion curves by using one-dimensional pseudo-homogeneous model of plug-flow isothermal reactor. The residual squared sum (RSS) between experimental data and model predictions was minimized (optimization criterion) and the square of correlation coefficient (R²) was calculated. The following margin values of the kinetics parameters were established: methane R² = 0.99, SD = ±3.6%; ethane R² = 0.99, SD = ±2.9%; propane R² = 0.99, SD = ±5.3%; and butane R² = 0.99, SD = ±4.0%. The obtained results are displayed in Figure 5.

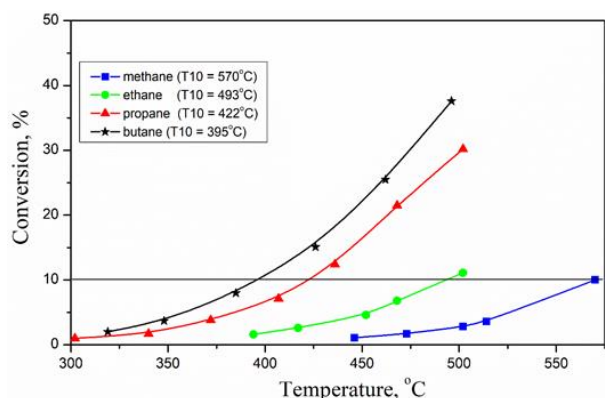


Fig. 5. Conversion-temperature dependence for complete oxidation of different hydrocarbons (methane, ethane, propane, and butane) over CuWO₄ catalyst.

It is seen that the highest temperature for 10% conversion was observed for methane combustion

(T₁₀ = 570 °C) due to the known stability of this compound. As it is well known [37], the highest temperature to achieve 10% conversion (T₁₀) is required for methane combustion and addition of carbon atoms to methane molecule and up to C₄ leads to a decrease in T₁₀. For our CuWO₄ catalyst, this reduction is higher than 170 °C from methane to *n*-butane.

To calculate pre-exponential factor (k_0) and apparent activation energy (E_{app}), data on conversion degrees below 45% were utilized. For such cases, calculated values for average effectiveness factor (accounting for irregular shaped catalyst particles) were within the limits of 0.95–0.99 and therefore the effect of internal diffusion effect had to be implemented in the reactor model by applying of iterative approach. Table 1 gives apparent activation energy values and the calculated rate constants for complete oxidation of the investigated hydrocarbons over CuWO₄ catalyst.

Table 1. Reaction parameters (pre-exponential factors k_0 and the apparent activation energies E_{app}), for the complete oxidation of hydrocarbons on CuWO₄ catalyst.

Hydrocarbon	k_0 , s ⁻¹	E_{app} , kJ/mol	ΔH_{C-H} , kJ/mol
methane	$2.08 \times 10^6 (\pm 1.0 \times 10^5)$	88.4 (±5)	433
ethane	$5.80 \times 10^6 (\pm 1.1 \times 10^5)$	86.0 (±4)	410
propane	$7.99 \times 10^6 (\pm 1.4 \times 10^5)$	80.5 (±4)	394
<i>n</i> -butane	$3.43 \times 10^6 (\pm 2.2 \times 10^5)$	73.0 (±3)	394

As can be seen the apparent activation energy are decreased from methane to butane, which could be correlated with the strength of the weakest H–C bond of the corresponding *n*-alkane [38,39]. It should be pointed out that a similar trend of decrease in apparent activation energy was reported earlier [40].

CONCLUSIONS

A single CuWO₄ phase was synthesized by thermal treatment at 400 °C of mechanically activated mixture of copper and tungsten oxides. Several effects were established during the ball milling processes including full amorphisation of the initial oxides, lack of chemical reaction after prolonged activation up to 20 h, and partial transformation of CuO to Cu₂O phase. The formation of amorphous phase favoured obtaining of CuWO₄ nanopowder of 24 nm crystallite size. The prepared nanostructured CuWO₄ was tested for possible application as catalyst for abatement of waste gases containing alkanes in a reactions of complete oxidation of C₁–C₄ hydrocarbons. The highest temperature for 10% conversion (T₁₀) was measured for methane, while one further carbon added the to the

C₁ hydrocarbon molecule led to a decrease in T10 by about 70 °C (from methane to propane) and further by 30 °C from propane to *n*-butane. Calculated apparent activation energies for the reaction of complete oxidation decreased from methane to *n*-butane, and this effect was associated decreased strength of the weakest C–H bond of the corresponding alkane.

REFERENCES

1. P. Schmitt, N. Brem, S. Schunk, C. Feldmann, *Adv. Funct. Mater.*, **21**, 3037 (2011).
2. S. J. Naik, A. V. Salker, *Catal. Commun.*, **10**, 884 (2009).
3. E. L. S. Souza, J. C. Sczancoski, I. C. Nogueira, M. A. P. Almeida, M. O. Orlandi, M. S. Li, R. A. S. Luz, M. G. R. Filho, E. Longo, L. S. Cavalcante, *Ultrasonic Sonochem.*, **38**, 256 (2017).
4. S. M. Pourmortazavi, M. Rahimi-Nasrabadi, M. Khalilian-Shalamazi, H. R. Chaeni, S. S. Hajimirsadeghi, *J. Inorg. Organomet. Polym.*, **22**, 333 (2014).
5. M. A. Damian, Y. Rodriguez, J. L. Solis, W. Estrada, *Thin Solid Film*, **444**, 104 (2003).
6. M. V. Lalic, Z. S. Popovic, F. R. Vukajlovic, *Comp. Mater. Sci.*, **50**, 1179 (2011).
7. K. Sieber, R. Kershaw, K. Dwight, A. Wold, *Inorg. Chem.*, **22**, 2667 (1983).
8. L. Kihlberg, E. Geber, *Acta Cryst. B*, **26**, 1020 (1970).
9. O. Yu. Khyzhuna, T. Strunskusb, S. Crammc, Yu. M. Solonina, *J. Alloys Compnd.*, **389**, 14 (2005).
10. J. Timoshenko, A. Anspoks, A. Kalinko, A. Kuzmin, *Phys. Scr.*, **89**, 044006 (2014).
11. O. Yu. Khyzhun, V.L. Bekenev, Yu.M. Solonin, *J. Alloys Compnd.*, **480**, 184 (2009).
12. R. Ruiz-Fuertes, A. Friedrich, J. Pellicer-Porres, D. Errandonea, A. Segura, W. Morgenroth, E. Haussuhl, C.-Y. Tu, A. Polian, *Chem. Mater.*, **23**, 4220 (2011).
13. D. Kumar, S. Karuppuchamy, *Ceram. Inter.*, **40**, 12397 (2014).
14. S. M. Pourmortazavi, M. Rahimi-Nasrabadi, Y. Fazli, M. Mohammad-Zadeh, *Int. J. Refract. Met. Hard Mater.*, **51**, 29 (2015).
15. S. Kannan, K. Mohanraj, G. Sivakumar, *Chem. Select*, **2**, 4484 (2017).
16. T. Raghua, R. Sundaresan, P. Ramakrishnan, T. R. Rama Mohan, *Mater. Sci. Engin. A*, **304–306**, 438, (2001).
17. A. F. Fuentes, L. Takacs, *J. Mater. Sci.*, **48**, 598 (2013).
18. X. Cuo, D. Xiang, G. Duan. P. Mou, *Waste Manage.*, **30**, 4 (2010).
19. Y. Dimitriev, M. Gancheva, R. Iordanova, *J. Alloys Compd.*, **519**, 161 (2012).
20. M. Mancheva, R. Iordanova, D. Klissurski, G. Tyuliev, B. Kunev, *J. Phys. Chem. C*, **111**, 1101 (2007).
21. M. Mancheva, R. Iordanova, Y. Dimitriev, *J. Alloys Compd.*, **509**, 15 (2011).
22. R. Iordanova, M. Mancheva, Y. Dimitriev, D. Klissurski, G. Tyuliev, B. Kunev, *J. Alloys Compd.*, **485**, 104 (2009).
23. M. Gancheva, R.Iordanova, Y. Dimitriev, D. Nihtianova, P. Stefanov, A. Naydenov, *J. Alloys Compd.*, **570**, 34 (2013).
24. M. Gancheva, A. Naydenov, R. Iordanova, D. Nihtianova, P. Stefanov, *J. Mater. Sci.*, **50**, 3447 (2015).
25. M. F. Daniel, B. Desbat, J. C. Lassegues, B. Gerand, M. Figlarz, *J. Solid State Chem.*, **67**, 235 (1987).
26. C. L. Veenas, L. R. Asitha, V. C. Bose, A. S. A. Raj, G. Madhu, V. Biju, *Mater. Sci. Engin.*, **73**, 012119 (2015).
27. S. Wang, H. Xu, L. Qian, X. Jia, J. Wang, Y. Liu, W. Tang, *J. Solid State Chem.*, **182**, 1088 (2009).
28. K. Borgohain, J. B. Singh, M. V. Rama Rao, T. Shripahi, S. Mahamuni, *Phys. Rev.*, **61**, 11093 (2000).
29. M. Kouti, L. Matouri, *Transaction F, Nanotechnology*, **17**, 73 (2010).
30. C. Wei, Y. Huang, X. Zhang, X. Chen, J. Yan, *Electrochim. Acta*, **220**, 156 (2016).
31. G. M. Clark, W. P. Doyel, *Spectrochim. Acta*, **22**, 1441 (1966).
32. O. Yu. Khyzhun, V. L. Bekenev, Yu. M. Solonin, *J. Alloys Compd.*, **480**, 184 (2009).
33. V. V. Fomichev, O. I. Kondratov, *Spectrochim. Acta A*, **50**, 1113 (1994).
34. M. Daturi, G. Busca, M. M. Borel, A. Leclaire, P. Piaggio, *J. Phys. Chem.*, **101**, 4358 (1997).
35. F. Duprat, *Chem. Eng. Sci.*, **57**, 901 (2002).
36. P. Harriot, *Chemical Reactor Design*, Marcel Dekker, Inc., 2003.
37. F. G. Dwyer, *Catal. Rev. Sci. Eng.*, **6**, 261 (1972).
38. M. Zboray, A. T. Bell, E. Iglesia, *J. Phys. Chem. C*, **113**, 12380 (2009).
39. P. Deshlahra, E. Iglesia, *J. Phys. Chem. C*, **120**, 16741 (2016).
40. Y. Xin, H. Wang, C. K. Law, *Combust. Flame*, **161**, 1048 (2014).
41. L. Van De Beld, M. P. G. Bijl, A. Reinders, B. Van Der Werf, K. R. Westerterp, *Chem. Eng. Sci.*, **49**, 4361 (1994).

МЕХАНОХИМИЧЕН АКТИВИРАН ТВЪРДОФАЗЕН СИНТЕЗ И КАТАЛИТИЧНИ СВОЙСТВА НА CuWO₄

М. Н. Ганчева*, П. М. Конова, Г. М. Иванов, Л. И. Александров, Р. С. Йорданова,
А. И. Найденов

*Институт по обща и неорганична химия, Българска академия на науките,
ул. „Акад. Георги Бончев“, бл. 11, 1113 София, България*

Постъпила на: 16 януари 2018 г.; Преработена на: 26 април 2018 г.

(Резюме)

Изучено е получаването и каталитичните свойства на наноструктуриран меден волфрамат. Смес от CuO и WO₃ в молно отношение 1:1 бе подложена на механохимично активиране на въздух използвайки планетарна топкова мелница за различен период от време. Структурните и фазовите трансформации бяха проследени чрез рентгенофазов анализ, диференциален термичен анализ (ДТА) и инфрачервена спектроскопия. Механохимичното третиране доведе до прогресивно аморфизиране на изходните оксиди. Пълна аморфизация бе осъществена след 7 часа механохимична обработка и се запази до 20 часа време на активиране. ДТА на аморфния образец показва, че температурата на кристализация е 430 °С. Монофазен наноструктуриран CuWO₄ бе синтезиран след термична обработка на аморфната фаза при 400 °С. CuWO₄ бе тестван в реакция на пълно каталитично окисление на C₁-C₄ въглеводороди, като най-високата температура за постигане на степен на превръщане 10% (T10) бе установена при метана, а добавянето на всеки следващ въглероден атом към метановата молекула води до понижаване на T10 с около 70 °С (от метан до пропан) и с около 30 °С от пропан до *n*-бутан. Изчислените стойности на наблюдаемата активираща енергия за реакцията на пълно каталитично окисление показва понижение в реда от метан до *n*-бутан, като ефектът е в корелационна зависимост от енергията за разкъсване на най-слабата C–H връзка в съответния въглеводород.